JCARME
ISSN: 2228-7922
Journal of Computational and Applied Research in Mechanical Engineering
Vol. 8, No. 1, pp. 49-60
jcarme.sru.ac.ir


# Torsional analysis of an orthotropic long cylinder weakened by multiple axisymmetric cracks

**A. R. Hassani[a], A. Hassani[a,*] and M. M. Monfared[b]**

*[a]Young Researchers and Elite Club, Hashtgerd Branch, Islamic Azad University, Alborz, Iran.*
*[b]Department of Mechanical Engineering, Hashtgerd Branch, Islamic Azad University, P.O. Box 33615-178, Alborz, Iran.*

**Article info:**
Received: 03/02/2017
Accepted: 13/05/2018
Online: 13/05/2018

**Keywords:**
Rotational somigliana ring dislocation,
Torsion,
Long cylinder,
Orthotropic,
Axisymmetric cracks,
Dislocation density.

**Abstract**
The solution to the problem of an orthotropic long cylinder subjected to torsional loading is first obtained by means of separation valuables. The cylinder is twisted by two lateral shear tractions, and the ends of the cylinder surface of the cylinder are stress-free. First, the domain under consideration is weakened by an axisymmetric rotational Somigliana ring dislocation. The dislocation solution is employed to derive a set of Cauchy singular integral equations for the analysis of multiple axisymmetric planner cracks. The numerical solution to these integral equations is used to determine the stress intensity factors for the tips of the concentric planar cracks. A preliminary comparison between results of this study and those available in the literature is performed to confirm the validity of the proposed technique. Several examples of multiple concentric planner cracks are solved and graphically displayed. Furthermore, the configuration of the cracks and the interaction between cracks is studied.

## 1. Introduction

Shafts in a machine are bars to hold or turn other parts that move or spin. Due to the simplicity of manufacturing, they are generally produced in the form of the bars with a circular cross-section. Shafts are often subjected to torsion in the process of working; therefore, cracking is one of their major issues. Some papers that analytically deal with the circular bars with no defects are as follows:
The torsion problem of two dissimilar half-spaces made of homogeneous materials and bonded through a thin layer of functionally graded material (FGM) interfacial region, was treated by Ozturk and Erdogan [1]. There was an axisymmetric penny-shaped crack in the interface between the lower half-space and the FGM thin layer. A problem similar to the above-mentioned paper was re-examined by Xuyue et al. [2], which the penny-shaped crack was inside the interfacial FGM layer. The problem was also solved by the method similar to that of used in Ref. [1].
Study of the way in which bi-materials are constructed makes it possible to introduce a very thin layer of an FGM between two distinctly different materials. Xuyue et al. [3] treated the problem of a penny-shaped crack in such an interfacial zone, along with the thickness of

*Corresponding author
*email address: a.hassani1111@gmail.com*

which the elastic modulus is varied in the power form of a linear function of thickness variable.
Danyluk and Singh [4] investigated the problem of an infinite solid containing a flat annular crack subjected to an axial torsion. Using Hankel transform, the solution of the problem was reduced to triple-integral equations containing Bessel functions of order 1 wherein the equations were written for the surface of the crack beside the inner and the outer regions of it.
The problem of axially symmetric torsion for two bonded dissimilar FGM elastic layers with an interfacial penny-shaped crack was the subject of a study done by Saxena et al. [5]. A multilayered laminated composite with an interfacial penny-shaped crack under a symmetric torsion around the axis normal to interface was the subject of the study by Hemed and Dhaliwal [6]. Fildis and Yahsi [7] investigated the axisymmetric problem of two homogeneous half-spaces bonded to each other through a non-homogeneous interfacial region with a penny-shaped crack. By the use of the Hankel transform, the problem was reduced to a singular integral equation. The numerical solution of the singular integral equation yielded the corresponding stress intensity factor of the crack tip. The problem of a bi-material infinite domain subjected to torsional loading weakened by a Mode III interfacial cylindrical crack was treated by Demir and Khraishi [8].
As a relatively different problem of those reviewed in the above paragraphs, the interaction between a spherical inclusion and a penny-shaped crack located on an infinite elastic body was studied by Godin [9]. Chang [10] used the Hankel transform and the Fourier series to analyze the torsion problem of a finite cylinder containing a concentric penny-shaped crack. Finally, the numerical results of the stress intensity factor of the crack tip were given. Zhang [11] re-examined the above-mentioned problem for a finite orthotropic cylinder with a concentric penny-shaped crack.
Torsion problem of a concentric penny-shaped crack off the middle plane of a finite isotropic cylinder was treated by Zhang and Zhang [12]. Using a similar technique of solution, the above problem was retreated by Zhang [13] for a concentric penny-shaped crack away from the middle plane of a finite orthotropic cylinder. By applying the Hankel transform and the Fourier series, the problem of an FGM finite cylinder with a concentric penny-shaped crack was studied by Liang and Zhang [14].
A problem of a penny-shaped or an annular crack in an FGM infinite cylinder subjected to torsional loading was solved by Xue-Li and Duo [15]. Akiyama et al. [16] solved the torsion problem of an infinite cylinder with two or an infinite number of concentric parallel penny-shaped cracks. The cracks were spaced apart in equal distances of each other. At the end step, the stress intensity factors of the crack tips were calculated. Malits [17] studied the torsion problem of a finite elastic cylinder with a circumferential edge crack. Using the exact asymptotic expansions of the solution of this equation, the stress intensity factor, as well as the torque, was derived for the case of a shallow crack.
To the best of authors' knowledge, the study presented in this article is a new attempt to analyze an orthotropic long cylinder with all kinds of arbitrary located axisymmetric cracks. It should be mentioned that Mode III is considered in this paper because of net torsion (see [2, 3, 11-14, 18-22]). In this paper, the classical theory of elasticity for fracture analysis of an orthotropic long cylinder containing a rotational Somigliana ring dislocation is first presented (Section 2). Next, the stress field of an intact long cylinder plane under torsional loading is studied (Section 3). Methodologically, Buckner’s principle can be used to study a long cylinder containing a set of coaxial axisymmetric cracks using results of Sections 2 and 3. This approach is presented in Section 4. Namely, a distributed dislocation method is employed to achieve a set of integral equations of Cauchy singular type. Subsequently, a set of relationships for the calculation of stress intensity factors are presented in terms of dislocation density. Finally, a method for solving the ensuing integral equations is recommended following the work of Faal et al. [23], where the solution of Erdogan et al. [24] is generalized so that both embedded and circumferential edge cracks can be taken into account simultaneously. Numerical examples will graphically be

displayed to demonstrate the effectiveness of the proposed solutions, as well as to understand the effect of position, geometry and also interaction between the cracks on the stress intensity factors at crack tips (Section 5). Finally, Section 6 offers concluding remarks.

## 2. Problem formulation

The only non-zero displacement component $u_\theta(r,z)$ which is independent of the angle $\theta$ is considered. Only the two nontrivial stress components prevail in this problem as follows [25]:

$$\tau_{r\theta} = G_{r\theta}\left(\frac{\partial u_\theta}{\partial r} - \frac{u_\theta}{r}\right) \quad (1)$$
$$\tau_{\theta z} = G_{\theta z}\frac{\partial u_\theta}{\partial z}$$

where $G_{r\theta}, G_{\theta z}$ are the orthotropic shear moduli of the cylinder. Substituting the expressions of Eq. (1) into the equilibrium equation $\frac{\partial \tau_{r\theta}}{\partial r} + \frac{\partial \tau_{\theta z}}{\partial z} + \frac{2}{r}\tau_{r\theta} = 0$, in the absence of body forces, leads to:

$$\frac{\partial^2 u_\theta}{\partial r^2} + \frac{1}{r}\frac{\partial u_\theta}{\partial r} + G^2\frac{\partial^2 u_\theta}{\partial z^2} - \frac{u_\theta}{r^2} = 0 \quad (2)$$

where $G^2 = G_{\theta z}/G_{r\theta}$. We consider an infinite cylinder with radius $R$, Fig. 1. The curved surface of the cylinder is kept stress-free.

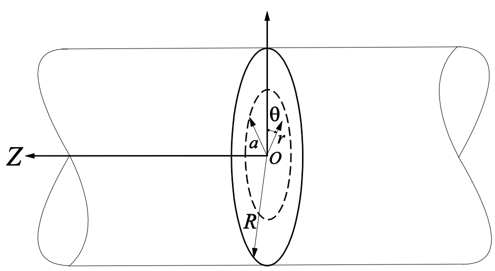


**Fig. 1.** Schematic view of an infinite cylinder with a rotational Somigliana ring dislocation.

A rotational Somigliana ring dislocation is located at $r = a$, $z = 0$ in the infinite cylinder under consideration, in which the radial cut of the dislocation is a circle $(r \leq a)$. Because of the anti-symmetry of this torsion problem, the displacement components in the radial and axial directions are vanished throughout the intact cylinder.

The only non-zero displacement component $u_\theta(r,z)$ which is independent of the angle $\theta$ is considered. The boundary condition along the curved surface reads as:

$$\tau_{r\theta}(R,z) = 0 \quad (3)$$

The condition representing a rotational Somigliana ring dislocation located at $r = a$, $z = 0$ in an long cylinder with the cut of dislocation in radial direction is:

$$u_\theta(r,0^+) - u_\theta(r,0^-) = \frac{b_\theta a}{r}H(r-a) \quad (4)$$

where, $b_\theta a/r$ designates the magnitude of the dislocation Burgers vectors and $H(.)$ is the Heaviside step-function. Generally, the relative displacement of the dislocation cut edges is considered to be constant. Here for simplicity of the solution, a cut with a variable relative displacement of its edges is defined. Moreover, the continuity of the traction vector on the cut of the dislocation requires that:

$$\tau_{\theta z}(r,0^+) = \tau_{\theta z}(r,0^-) \quad (5)$$

For a rotational Somigliana ring dislocation, the problem is antisymmetric with respect to the plane $z = 0$. For the antisymmetric problem, the half-space $z > 0$ is subjected to the following boundary condition:

$$u_\theta(r,0^+) = \frac{b_\theta a}{2r}H(r-a) \quad (6)$$

Using the technique of separation of variables, for $z > 0$ a solution to Eq. (2) is proposed as:

$$u_\theta(r,z) = \int_0^\infty A(\xi)I_1(G\xi r)sin(\xi z)d\xi + \int_0^\infty B(\eta)e^{-\eta z}J_1(G\eta r)d\eta \quad (7)$$

where $A(\xi)$ and $B(\eta)$ are unknown coefficients which must be determined using the boundary conditions (12) and (15). Also $J_1(.)$ and $I_1(.)$ are the Bessel function and the modified Bessel function of first kind of order 1, respectively. Using the constitutive Eqs. (1 and 7), the stress components are readily written as:

$$\tau_{r\theta}(r,z) = G_{r\theta}G\left(\int_0^\infty \xi A(\xi)I_2(G\xi r)sin(\xi z)d\xi - \int_0^\infty \eta B(\eta)e^{-\eta z}J_2(G\eta r)d\eta\right)$$
$$\tau_{\theta z}(r,z) = G_{\theta z}G\left(\int_0^\infty \xi A(\xi)I_1(G\xi r)cos(\xi z)d\xi - \int_0^\infty \eta B(\eta)e^{-\eta z}J_1(G\eta r)d\eta\right) \quad (8)$$

Satisfying the boundary condition $\tau_{r\theta}(R,z) = 0$ implies that:

$$G\xi A(\xi)I_2(G\xi R) = \frac{2}{\pi}\int_0^\infty \eta B(\eta)J_2(G\eta R)\left(\int_0^\infty e^{-\eta z}sin(\xi z)dz\right)d\eta \quad (9)$$

Integrating of above relation with respect to $z$, results in:

$$A(\xi) = \frac{2}{G\pi I_2(G\xi R)}\int_0^\infty \frac{\eta B(\eta)J_2(G\eta R)}{\eta^2+\xi^2}d\eta \quad (10)$$

Applying the boundary condition (6) to the solution (8) yields:

$$\int_0^\infty B(\eta)J_1(G\eta r)d\eta = \frac{b_\theta a}{2r}H(r-a) \quad (11)$$

Making the use of the inverse Hankel transform, the solution to the Eq. 11 is readily written as:

$$B(\eta) = \frac{b_\theta a}{2}\eta\int_0^\infty H(\tau-a)J_1(G\eta\tau)d\tau = \frac{b_\theta a}{2G}J_0(G\eta a) \quad (12)$$

By replacing the coefficient $B(\eta)$ in Eq. (10) by $\frac{b_\theta a}{2G}J_0(G\eta a)$ it can be approached as [26]:

$$A(\xi) = \frac{b_\theta a}{G\pi I_2(G\xi R)}\left[\frac{2}{G^2R^2\xi^2} - K_2(GR\xi)I_0(G\tau\xi)\right] \quad (13)$$

By substituting the coefficients $B(\eta)$ and $A(\xi)$ form Eqs. (12 and 13) into Eq. (8), the stress components for $z > 0$ take the form:

$$\tau_{r\theta}(r,z) = \frac{b_\theta a G_{r\theta}}{\pi}\int_0^\infty \frac{\xi I_2(G\xi r)}{I_2(G\xi R)}\left[\frac{2}{G^2R^2\xi^2} - I_0(Ga\xi)K_2(GR\xi)\right]sin(\xi z)d\xi - \frac{b_\theta a G_{r\theta}}{2}\int_0^\infty \eta e^{-\eta z}J_0(\eta Ga)J_2(\eta Gr)d\eta \quad (14)$$
$$\tau_{\theta z}(r,z) = \frac{b_\theta a G_{\theta z}}{\pi}\int_0^\infty \frac{\xi I_1(G\xi r)}{I_2(G\xi R)}\left[\frac{2}{G^2R^2\xi^2} - I_0(aG\xi)K_2(RG\xi)\right]cos(\xi z)d\xi - \frac{b_\theta a G_{\theta z}}{2}\int_0^\infty \eta e^{-\eta z}J_0(\eta aG)J_1(\eta Gr)d\eta$$

To extend the stress fields for $z < 0$, in the second integrals of the above relations $z$ is replaced by $|z|$. The second integral of $\tau_{r\theta}(r,z)$ is multiplied by $sgn(z)$ which refers to the sign function. Using the Mathematica 10, the stress component $\tau_{\theta z}(r,z)$ at middle plane of the cylinder i.e. $z = 0$, is simplified as follows:

$$\tau_{\theta z}(r,0) = \frac{b_\theta a G_{\theta z}}{\pi}\int_0^\infty \frac{\xi I_1(G\xi r)}{I_2(G\xi R)}\left[\frac{2}{G^2R^2\xi^2} - I_0(aG\xi)K_2(RG\xi)\right]d\xi - \frac{b_\theta a G_{\theta z}}{\pi G^2}\begin{cases}\frac{1}{r^2-a^2}\boldsymbol{E}\left(\frac{a}{r}\right) & r > a \\ \frac{1}{ar}\left(\boldsymbol{K}\left(\frac{r}{a}\right) + \frac{a^2}{r^2-a^2}\boldsymbol{E}\left(\frac{r}{a}\right)\right) & r < a\end{cases} \quad (15)$$

where $\boldsymbol{K}(k) = \int_0^{\pi/2} dx/\sqrt{1-k^2sin^2x}$ and $\boldsymbol{E}(k) = \int_0^{\pi/2}\sqrt{1-k^2sin^2x}\,dx$ are the complete elliptic integrals of the first and second kind, respectively. As it can be seen easily, the stress component on the middle plane of the cylinder, $\tau_{\theta z}(r,0)$ has Cauchy-type singularity i.e. $\tau_{\theta z}(r,0)\sim\frac{1}{r-a}\ as\ r\to a$. This kind of singularity was previously reported for an infinite domain with rotational Somigliana ring dislocation [27].

### 3. Torsion of an intact infinite cylinder under lateral shear tractions

An infinite cylinder with height $2h$ and radius $R$, Fig. 2, is considered in which the flat surfaces of the cylinder, that is, $z=\pm h$ are stress-free. Also, the curved surface of the cylinder is left stress-free except for regions $d_1<z<d_2$ and $-d_2<z<-d_1$. In these regions the cylinder is under constant shear tractions $\tau_0$ and $-\tau_0$ which are applied in the opposite directions. In fact, the cylinder is subjected to two identical bidirectional torques as $M_0=2\pi R^2\tau_0(d_2-d_1)$ which are applied near the two ends of cylinder in the opposite directions. Because of the axisymmetry of the torsion problem, the displacement components in the radial and axial directions vanish throughout the intact cylinder.

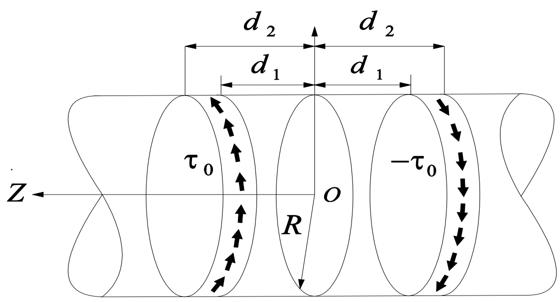


**Fig. 2.** An infinite cylinder under constant bidirectional shear tractions.

The problem is anti-symmetric with respect to the middle plane of the cylinder ($z=0$). The boundary conditions of the problem are as follow:

$$\tau_{\theta z}(r,\pm h)=0 \qquad (16)$$
$$\tau_{r\theta}(R,z)=\tau_0[H(z-d_1)-H(z-d_2)],\quad d_2>d_1$$

The solution to Eq. (2) may be readily found using the separation of variables technique. The following solution form is proposed for the problem:

$$u_\theta(r,z)=\int_0^\infty A(\xi)I_1(G\xi r)sin(\xi z)d\xi \qquad (17)$$

where $B_n$ is an unknown coefficient and $I_1(.)$ is the modified Bessel function of the first kind of order 1. By virtue of Eq. (1), the stress components read as:

$$\tau_{r\theta}(r,z)=G_{r\theta}G\int_0^\infty \xi A(\xi)I_2(G\xi r)sin(\xi z)d\xi \qquad (18)$$
$$\tau_{\theta z}(r,z)=G_{\theta z}G\int_0^\infty \xi A(\xi)I_1(G\xi r)cos(\xi z)d\xi$$

Using Eq. (1), the second boundary condition of (3) is applied as below:

$$\tau_{r\theta}(r,z)=G_{r\theta}G\int_0^\infty \xi A(\xi)I_2(G\xi R)sin(\xi z)d\xi=\tau_0[H(z-d_1)-H(z-d_2)] \qquad (19)$$

Taking the inverse Fourier sine transform of the above equation leads to:

$$A(\xi)=\frac{2\tau_0}{\xi^2 I_2(G\xi R)\pi G_{r\theta}}(cos(\xi d_1)-cos(\xi d_2)) \qquad (20)$$

Finally, the stress field arrives as:

$$\tau_{r\theta}(r,z)=\frac{2\tau_0}{\pi}\int_0^\infty \frac{I_2(\xi Gr)}{\xi I_2(\xi GR)}(cos(\xi d_1)-cos(\xi d_2))sin(\xi z)d\xi \qquad (21)$$
$$\tau_{\theta z}(r,z)=\frac{2\tau_0}{\pi}\int_0^\infty \frac{I_1(\xi Gr)}{\xi I_2(\xi GR)}(cos(\xi d_1)-cos(\xi d_2))cos(\xi z)d\xi$$

**4. Axisymmetric crack formulation**

Suppose an infinite cylinder is weakened by $N_p$ penny-shaped cracks, $N_a$ annular cracks and $N_c$ circumferential edge cracks in which all defects located concentrically in the cylinder. The radii of the penny-shaped cracks and the inner radii of the circumferential edge cracks are:
$c_j, j = 1,2,\dots,N_p$ and $d_j, j = N_p + N_a + 1, N_p + N_a + 2,\dots,N$, respectively, and the inner and outer radii of the annular cracks are $a_j$ and $b_j, j = N_p + 1,\dots,N_p + N_a$, respectively. Therefore, the number of all defects is $N = N_p + N_a + N_c$. The parametric form of the above-mentioned cracks can be written as:

$$\begin{aligned}
&r_j(s) = L_j(1-s),\\
&-1 \le s \le 1 \ \ for\ penny-shaped\ cracks\\
&r_j(s) = L_j s + 0.5(b_j + a_j),\\
&-1 \le s \le 1 \ \ for\ annular\ cracks\\
&r_j(s) = L_j s + 0.5(R + d_j),\\
&-1 \le s \le 1 \ \ for\ circumferential\\
&edge\ cracks
\end{aligned} \tag{22}$$

in which

$$L_j = 0.5 \begin{cases} c_j & for\ penny-shaped\ cracks\ (j = 1,2,\dots,N_p) \\ b_j - a_j & for\ annular\ cracks\ (j = N_p+1, N_p+2,\dots,N_p+N_a) \\ R - d_j & for\ circumferential\ edge\ cracks\ (j = N_p+N_a+1, N_p+N_a+2,\dots,N) \end{cases} \tag{23}$$

Let dislocations with unknown densities $b_{\theta j}(t)$ be distributed on the infinitesimal segment at the surface of the j-th concentric (penny shape or annular or circumferential edge) crack situated at $z = z_j$. Using Eq. (21), the traction component $\tau_{\theta z}(r_i(s), z_i), i = 1,2,\dots,N$ on the surface of the i-th crack caused by distributing of the dislocations on all surfaces of the cracks yields:

$$\tau_{\theta z}(r_i(s), z_i) = \sum_{j=1}^{N} \int_{-1}^{1} k_{ij}(s,t) b_{\theta j}(t)\, dt\, , i = 1,2,\dots,N \tag{24}$$

where the kernel of integrals $k_{ij}(s,t)$ are given by:

$$k_{ij}(s,t) = L_j\{\frac{r_j(t)\mu}{\pi}\int_0^{\infty} \frac{\xi I_1(\xi r_i(s))}{I_2(\xi R)}[\frac{2}{R^2\xi^2} - I_0(r_j(t)\xi)K_2(R\xi)]cos(\xi(z_i - z_j))d\xi - \frac{r_j(t)\mu}{2}\int_0^{\infty} \eta e^{-\eta|z_i - z_j|} J_0(\eta r_j(t)) J_1(\eta r_i(s)) d\eta\} \tag{25}$$

By virtue of Bueckner's principle [28] the left-hand side of Eq. (24), after changing the sign, is the traction caused by applying the torques on the intact finite cylinder at the presumed surfaces of the cracks. The applied traction on the intact infinite cylinder is taken to be as the second equation of Eq. (16), and its equalizer loading, as well as the resulting stress components, read as Eq. (21). The crack opening displacement by considering the definition of the dislocation density function is given by:

$$u_{\theta j}^{+}(s) - u_{\theta j}^{-}(s) = \frac{L_j}{r_j(s)}\int_{-1}^{s} r_j(t) b_{\theta j}(t)\, dt, \quad j = 1,2,\dots,N \tag{26}$$

It is known that the displacement field is single-valued away from the penny-shaped and annular crack surfaces. Therefore, the dislocation density for the j-th crack of these kinds must be subjected to the closure requirement as $\int_{-1}^{1} r_j(t) b_{\theta j}(t) dt = 0, j = 1,2,\dots,N$.
The Cauchy singular integral Eq. (26) and the closure equations for the penny-shaped and annular cracks, that is, $\int_{-1}^{1} r_j(t) b_{\theta j}(t) dt = 0$ are solved simultaneously to determine the dislocation density function. The stress fields have a square-root singularity at the crack tips [29]. For penny-shaped and edge cracks, the embedded crack tip is assumed at $t = -1$. Thus, the dislocation densities for each kind of the cracks, are taken as [23, 27-29]:

$$b_{\theta j}(t)=\frac{g_{aj}(t)}{\sqrt{1-t^2}} \quad (27)$$

*for penny-shaped and annular cracks*

$$b_{\theta j}(t)=g_{cj}(t)\sqrt{\frac{1-t}{1+t}}$$

$for\ circumferential\ edge\ cracks$

Viewing Eq. (27), the numerical solution of the integral Eq. (24), in conjunction with the closure requirement for penny-shaped and annular cracks i.e. $\int_{-1}^{1} r_j(t)b_{\theta j}(t)dt=0$, is carried out by minor generalization of the procedure developed in Ref. [23]. These integral equations are discretized at the collocation points $t_k=cos\left(\frac{2k-1}{2n}\pi\right), k=1,2,\dots,n$ and $s_r=cos\left(\frac{r}{n}\pi\right), r=1,2,\dots,n-1$. Because the number of ensuing algebraic equations is $Nn-N_c$ while the number of unknowns $g_{pj}(t_k), j=1,2,\dots,N_p$ and $g_{aj}(t_k), j=N_p+1,N_p+2,\dots,N_p+N_a$ and $g_{cj}(t_k), j=N_p+N_a+1,\dots,N$ is $Nn$, Eq. (24) is discretized at the new arbitrary distinct discrete point other than $s_r$ and $t_k$, that is, the point $s_{0c}=1$. Finally, the integral equations are reduced to the following system of $Nn$ linear algebraic equations:

$$\begin{bmatrix} \boldsymbol{H}_{11} & \boldsymbol{H}_{12} & \dots & \boldsymbol{H}_{1N} \\ \boldsymbol{H}_{21} & \boldsymbol{H}_{22} & \dots & \boldsymbol{H}_{2N} \\ \vdots & \vdots & \ddots & \vdots \\ \boldsymbol{H}_{N1} & \boldsymbol{H}_{N2} & \dots & \boldsymbol{H}_{NN} \end{bmatrix} \begin{Bmatrix} \{g_{pj}(t_k)\} \\ \{g_{aj}(t_k)\} \\ \{g_{cj}(t_k)\} \end{Bmatrix} = -\begin{Bmatrix} \{\tau_{\theta z}(r_i(s_r),z_i)\} \\ \{\tau_{\theta z}(r_i(s_r),z_i)\} \\ \{\tau_{\theta z}(r_i(s_r),z_i)\} \end{Bmatrix} \quad (28)$$

in which the entries of the matrix and the components of vectors are given at Ref. [23]. Stress intensity factors for the singular crack tips of other kinds of the cracks are already written as:

$$\begin{cases} k_{IIIL}=\dfrac{G_{r\theta}\sqrt{L_j}}{2}g_{zj}(-1) \\ k_{IIIL}=\dfrac{G_{r\theta}\sqrt{L_j}}{2}g_{zj}(+1) \end{cases} \quad (29)$$

$for\ annular\ cracks$

$$k_{III}=\frac{G_{r\theta}\sqrt{L_j}}{2}g_{zj}(-1)$$

$for\ penny-shaped\ cracks$

$$k_{III}=G_{r\theta}\sqrt{L_j}g_{zj}(+1)$$

$for\ circumferential\ edge\ cracks$

**5. Results and discussion**

Let us first validate our solution with the published results. To this end, the paper is furnished to the examples 1-5. The capabilities of the procedure are also demonstrated by solving two more examples (Examples 6 and 7), as follows:

*Example 1*

An isotropic elastic space with an annular crack is considered under pure torsion, that inner and outer radii of the crack are $a$ and $b$, respectively. Also, the surface of the crack is subjected to a constant twisting load $\tau_0$. The normalized stress intensity factors, $k_{III}/k_0$ are depicted, with an excellent agreement with Ref. [30], in Fig. 3, wherein $k_0=\tau_0\sqrt{b}$.

*Example 2*

In the second example of validation, an infinite space with one penny shape crack, under torsional loading, is considered. The shear stress resulting from the torsion is $\tau_0 r/R$, in which $\tau_0$ is constant, and also $r$ and $R$ are the radial general coordinate and the radius of the crack, respectively. In Ref. [31], the stress intensity factor (SIF) was normalized by devisor $\tau_0\sqrt{R}$. The normalized SIF was constant $(4\pi/3)$. Comparison of the results obtained from the normalized SIF of this study for a penny shaped-crack and those available in Ref. [31] shows an exact agreement. There is only one more coefficient $\sqrt{\pi}$ in definition of the stress intensity factor in Ref. [31] in comparison with the present work which is a well-known coefficient in the literature.

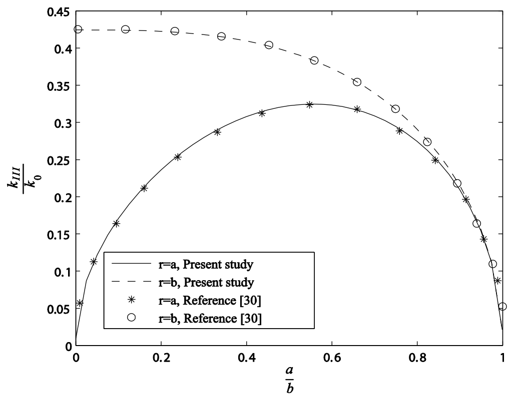


**Fig. 3.** Stress intensity factors for an annular crack in the elastic space.

*Example 3*

In another example of validation, an isotropic long cylinder with a radius $R$, weakened by a concentric penny-shaped crack with a radius $a$ is considered. The crack is subjected to torsional loading. The shear stress on the surface of the cracks has the same distribution of Example 2. Dimensionless stress intensity factors $k_{III}/k_0$, by assuming $k_0 = \frac{4\tau_0}{3}\sqrt{a/\pi}$ , are listed in Table 1 and is compared with those given in Ref. [32]. Also, the stress intensity factors of this paper must be multiplied by the coefficient$\sqrt{\pi}$. As it can be seen, there is good agreement between the results. Also, the stress intensity factor of the crack tip is increased by crack growth.

**Table 1.** Dimensionless stress intensity factors $k_{III}/k_0$ in term of $a/R$.

| $\frac{a}{R}$ | 0.1 | 0.2 | 0.3 |
|---|---|---|---|
| $k_{III}/k_0$ Present study | 1.000 | 1.0001 | 1.0006 |
| $k_{III}/k_0$ Ref. [32] | 1.000 | 1.002 | 1.007 |

*Example 4*

An infinite cylinder with radius $R$ weakened by a circular edge crack with the crack depth $R-a$ is considered. Table 2 gives a comparative analysis of the dimensionless stress intensity factor obtained by use of the present method and those attained by Refs. [17, 33]. The crack surface is under the constant moment $M$. The stress intensity factor is normalized with aid of a divisor $k_0 = \frac{2M\sqrt{R}}{\sqrt{\pi}a^3}$. As it can be seen from the tabulated results, the discrepancy is negligible. In this example, an additional coefficient $\sqrt{\pi}$ for the stress intensity factors must be considered. The stress intensity factor of the crack tip is initially enlarged by crack growth, and then it experiences a little reduction for deeper crack depth.

**Table 2.** Normalized stress intensity factors, for a circular edge crack in an infinite cylinder.

| $\frac{R-a}{R}$ | 0.05 | 0.1 | 0.2 |
|---|---|---|---|
| $k_{III}/k_0$ | 0.1987 | 0.2521 | 0.2914 |
| $k_{III}/k_0$ [17] | 0.199 | 0.252 | 0.292 |
| $k_{III}/k_0$ [33] | 0.210 | 0.231 | 0.274 |
| $k_{III}/k_0$ [33] | 0.2007 | 0.2552 | 0.2956 |

*Example 5*

An isotropic infinite long cylinder containing two concentric symmetric penny-shaped cracks is analyzed for validation with Ref. [16]. Any cross-section of the cylinder is subjected to a constant torsional load, $M$. The distance between the cracks is assumed to be $2h$ and radii of the cracks are $a$. Displayed in Fig. 4 are the variations of the non-dimensional SIF, $(k_{III}/k_0\,, k_0 = 2MR\sqrt{\pi R}/(\pi(R^4-b^4)))$, for two penny-shaped cracks versus $a/R$ and for different values of $h/R$. Also, the proposed relation of the SIF in this study must be multiplied by the coefficient$\sqrt{\pi}$.

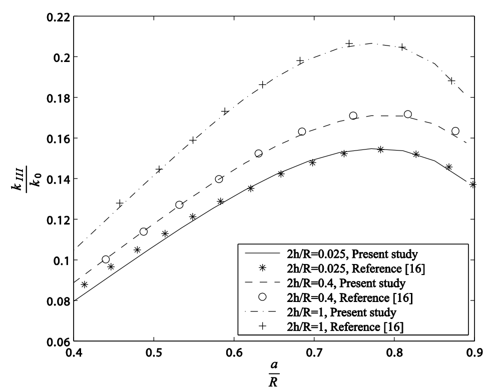


**Fig. 4.** Graph of the stress intensity factors with $a/R$ for two symmetric penny-shaped cracks.

*Example 6*

Torsion of a long cylinder with a penny-shaped crack, an annular crack and a circumferential edge crack in $z = 0$, as shown in Fig. 5, are considered. The stress field affecting the cracks which is resulted from the torsional loading is obtained by Eq. (21). The loading is specified by $d_1 = 2.5R,\ d_2 = 3h$. Center of the annular crack with inner and outer radii $a_1$ and $b_1$ is located at $r = 0.5R$. Additionally, $l$ is considered to be the half-length of the annular crack and the length of the edge crack.

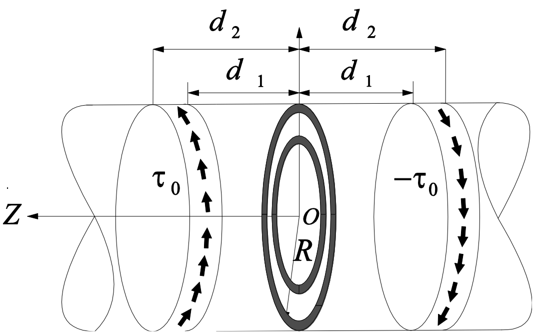


**Fig. 5.** A long cylinder with one annular crack one circumferential edge crack.

The normalized stress intensity factors, $k_{III}/k_0$ calculated by the dislocation method are plotted in Figs. 6 and Fig 7 in isotropic and orthotropic ($G = 1.2$) case, respectively, in which $k_0 = \tau_0\sqrt{R}$. It can be observed that the normalized stress intensity factors for all the tips of the cracks roughly increase with increasing the length of the cracks. Also, the interaction between the crack tips is significant. The stress intensity factor grows as the distance between the crack tips reduces.

*Example 7*

As a final example, a long cylinder with the of edge two annular cracks in $z = 0$ is considered. Center of the annular cracks are situated at $r = 0.25R$ and $r = 0.75R$, respectively, as shown in Fig 8. The curves, shown in the Figs. 8 and 9, display variation of the dimensionless stress intensity factors corresponding to the dimensionless half-length of the cracks for the isotropic and orthotropic cases. The figure shows that stress intensity factors for all of the crack tips increase rapidly with growing crack length, because of the interaction of the singular crack tips.

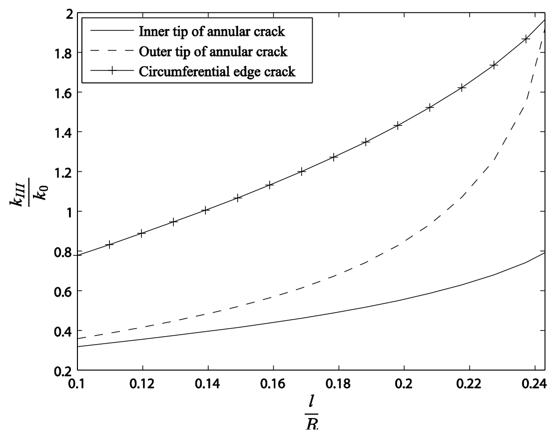


**Fig. 6.** Variation of the dimensionless stress intensity factor versus the crack length in isotropic case.

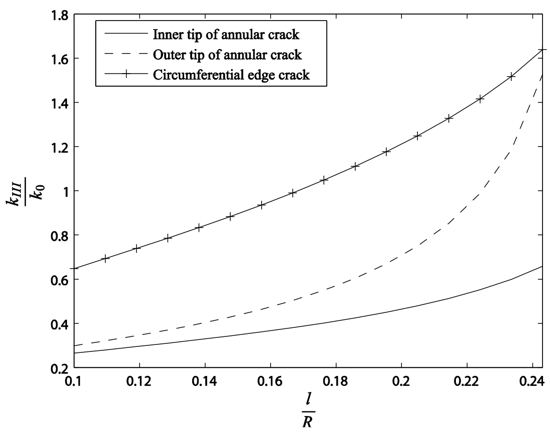


**Fig. 7.** Variation of the dimensionless stress intensity factor versus the crack length in orthotropic case.

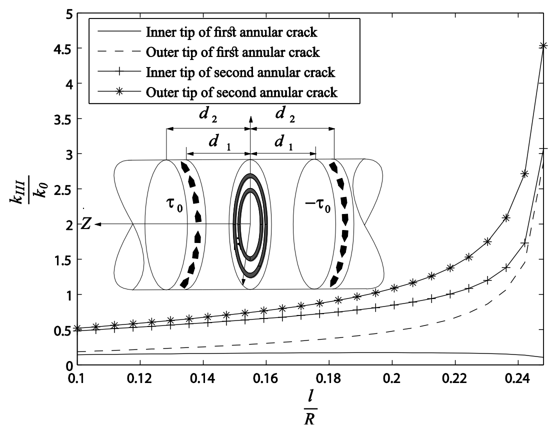


**Fig. 8.** Variation of the dimensionless stress intensity factor versus the crack length in isotropic case.

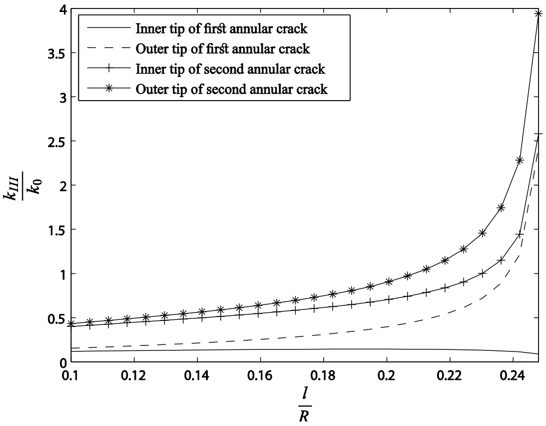


**Fig. 9.** Variation of the dimensionless stress intensity factor versus the crack length in orthotropic case.

## 6. Conclusions

A solution of the problem of an orthotropic long cylinder plane subjected to torsional loading weakened by a rotational Somigliana ring dislocation is first presented in terms of dislocation densities. Consequently, the stress field in an aforementioned region under torsion is given. The dislocation densities on the cracks surfaces are obtainable by solving a set of integral equations of Cauchy singular type. Finally, the distributed dislocation technique is used to solve the problems with multiple axisymmetric cracks. Some numerical examples about the variation behavior of stress intensity factors are given to study the effects of the geometry of the cracks, interactions between the crack tips and distance of the crack tip from traction free surface. In summary, the stress of crack tips in circular planes can depend on critical factors such as the distance of the crack tip from the free boundary of the circular region and the location of traction.

## References

[1] M. Ozturk, F. Erdogan, An Axisymmetric Crack in Bonded Materials With a Nonhomogeneous Interfacial Zone Under Torsion, *Journal of Applied Mechanics*, Vol. 62, No. 1, pp. 116-125, (1995).

[2] W. Xuyue, Z. Zhenzhu, W. Duo, On the penny-shaped crack in a nonhomogeneous interlayer of adjoining two different elastic materials, *International Journal of Solids and Structures*, Vol. 34, pp. 3911-3921, (1997).

[3] W. Xuyue, Z. Zhenzhu, W. Duo, On the penny-shaped crack in a non-homogeneous interlayer under torsion, *International Journal of Fracture*, Vol. 82 No. 4, pp. 335-343, (1996).

[4] H. T. Danyluk, B. M. Singh, Problem of an infinite solid containing a flat annular crack under torsion, *Engineering Fracture Mechanics*, Vol. 24, No. 1, pp. 33-38, (1986).

[5] H. S. Saxena, R. S. Dhaliwal, W. He, J. G. Rokne, Penny-shaped interface crack between dissimilar nonhomogeneous elastic layers under axially symmetric torsion, Acta Mechanica, Vol. 99, No. 1, pp. 201-211, (1993).

[6] H. K. Hemed, R.S. Dhaliwal, Penny-shaped interface crack in a non-homogeneous multilayered medium under axially symmetric torsion, ZAMM - *Journal of Applied Mathematics and Mechanics*, Vol. 81, No. 3, pp. 205-211, (2001).

[7] H. Fildiş, O. S. Yahşi, The mode III axisymmetric crack problem in a non-homogeneous interfacial region between homogeneous half-spaces, *International Journal of Fracture*, Vol. 85, pp. 35-45, (1997).

[8] I. Demir, T. A. Khraishi, The Torsional Dislocation Loop and Mode III Cylindrical Crack, *Journal of Mechanics*, Vol. 21, No. 1, pp. 109-116, (2011).

[9] Y. Godin, The interaction between a penny-shaped crack and a spherical inclusion under torsion, *Zeitschrift für angewandte Mathematik und Physik ZAMP*, Vol. 46, No. 6, pp. 932-945, (1995).

[10] S. S. Chang, The general solution of a finite cylinder with a concentric penny-shaped crack under torsion, *Engineering Fracture Mechanics*, Vol. 22, No. 4, pp. 571-578, (1985).

[11] X. S. Zhang, The general solution of a finite orthotropic cylinder with a concentric penny-shaped crack under

torsion, *Engineering Fracture Mechanics*, Vol. 31, No. 5, pp. 827-835, (1988).

[12] X. S. Zhang, Y. U. Zhang, A concentric penny-shaped crack off the middle plane of a finite orthotropic cylinder under torsional shear stress, *Engineering Fracture Mechanics*, Vol. 31, No. 3, pp. 385-393, (1988).

[13] X. S. Zhang, Off-plane concentric penny-shaped crack in a finite cylinder under arbitrary torsion, Theoretical and Applied Fracture Mechanics, Vol. 9, No. 3, pp. 263-270, (1988).

[14] B. Liang, X. S. Zhang, The problem of a concentric penny-shaped crack of mode III in a nonhomogeneous finite cylinder, *Engineering Fracture Mechanics*, Vol. 42, No. 1, pp. 79-85, (1992).

[15] H. Xue-Li, W. Duo, A circular or ring-shaped crack in a nonhomogeneous cylinder under torsional loading, *International Journal of Fracture,* Vol. 68, No. 3, pp. R79-R83, (1994).

[16] T. Akiyama, T. Hara, T. Shibuya, Torsion of an Infinite Cylinder with Multiple Parallel Circular Cracks, *Theoretical and Applied Mechanics Letters*, Vol. 50, pp. 137-143, (2001).

[17] P. Malits, Torsion of a cylinder with a shallow external crack, *International Journal of Solids and Structures*, Vol. 46, No. 16, pp. 3061-3067, (2009).

[18] A. N. Zlatin, Y. S. Uflyand, Torsion of an elastic cylinder slackened by an external circular notch II. The case of a finite cylinder, *Journal of Elasticity*, Vol. 13, No. 2, pp. 215-223, (1983).

[19] I. N. Zlatina, Application of dual integral equations to the problem of torsion of an elastic space, weakened by a conical crack of finite dimensions, *Journal of Applied Mathematics and Mechanics,* Vol. 36, No. 6, pp. 1062-1068, (1972).

[20] H. Z. Hassan, Torsion of a non-homogeneous infinite elastic cylinder slackened by a circular cut, *Journal of Engineering Mathematics*, Vol. 30, No. 5, pp. 547-555, (1996).

[21] S. Kazuyoshi, S. Toshikazu, K. Takashi, The torsion of an infinite hollow cylinder with an external crack, *International Journal of Engineering Science*, Vol. 16, No. 10, pp. 707-715, (1978).

[22] T. Shibuya, T. Koizumi, T. Okuya, The Axisymmetric Stress Field in an Infinite Solid Cylinder with an External Crack under Torsion, Bulletin of JSME, Vol. 22, No. 249, pp. 1049-1052, (1979).

[23] R. T. Faal, S. J. Fariborz, H. R. Daghyani, Antiplane deformation of orthotropic strips with multiple defects, *Journal of Mechanics of Materials and Structures*, Vol. 1, No. 7, pp. 1097-1114, (2006).

[24] F. Erdogan, G. D. Gupta, T. S. Cook, *Numerical solution of integral equations. In: Sih, G. C. (Ed.), Methods of Analysis and Solution of Crack Problems*, Noordhoof, Leyden, Holland, (1973).

[25] J. Q. Tarn, Y. M. Wang, Fundamental solutions for torsional problems of a cylindrical anisotropic elastic medium, *Journal of the Chinese Institute of Engineers*, Vol. 9, No. 1, pp. 1-8, (1986).

[26] W. Magnus, F. Oberhettinger, R. P. Soni, *Formulas and theorems for the special functions of mathematical physics*, Berlin, (1966).

[27] E. Asadi, S. J. Fariborz, M. Ayatollahi, Analysis of multiple axisymmetric annular cracks, *Journal of Mechanics of Materials and Structures*, Vol. 4, No. 1, pp. 1-11, (2009).

[28] D. A. Hills, P. A. Kelly, D. N. Dai, A. M. Korsunsky, *Solution of Crack Problems: The Distributed Dislocation Technique*, Springer, (1996).

[29] I. N. Sneddon, M. Lowengrub, *Crack problems in the classical theory of elasticity*, Wiley, (1969).

[30] I. Choi, R. T. Shield, A note on a flat toroidal crack in an elastic isotropic body, *International Journal of Solids and Structures*, Vol. 18, No. 6, pp. 479-486, (1982).

[31] J. P. Benthem, W. T. Koiter, *Asymptotic approximations to crack problems, in: G. Sih (Ed.) Methods of analysis and solutions of crack problems*, Springer Netherlands, pp. 131-178, (1973).

[32] W. Qizhi, SIF solutions of a cylinder with a concentric penny-shaped crack under various loading conditions, *International Journal of Fracture*, Vol. 74, pp. R65-R70, (1995).

[33] B. A. Kudriavtsev, V. Z. Parton, Torsion and extension of a cylinder with an external annular slit, *Journal of Applied Mathematics and Mechanics*, Vol. 37, No. 2, pp. 297-306, (1973).

**How to cite this paper:**

A. R. Hassani, A. Hassani and M. M. Monfared,“ Torsional analysis of an orthotropic long cylinder weakened by multiple axisymmetric cracks” *Journal of Computational and Applied Research in Mechanical Engineering*, Vol. 8, No. 1, pp. 49-60, (2018).

**DOI:** 10.22061/jcarme.2018.2283.1214

**URL:** http://jcarme.sru.ac.ir/?_action=showPDF&article=830